Hindawi
Complexity
Volume 2021, Article ID 9398333, 17 pages
https://doi.org/10.1155/2021/9398333

Research Article

Results for Chaos Synchronization with New Multi-Fractional Order of Neural Networks by Multi-Time Delay

Fatin Nabila Abd Latiff and Wan Ainun Mior Othman

Institute of Mathematical Sciences, Universiti Malaya, Kuala Lumpur 50603, Malaysia

Correspondence should be addressed to Fatin Nabila Abd Latiff; fatin_nabilaa@yahoo.com and Wan Ainun Mior Othman; wanainun@um.edu.my

Received 2 November 2021; Accepted 9 December 2021; Published 30 December 2021

Academic Editor: Inés P. Mariño

A new finding is proposed for multi-fractional order of neural networks by multi-time delay (MFNNMD) to obtain stable chaotic synchronization. Moreover, our new result proved that chaos synchronization of two MFNNMDs could occur with fixed parameters and initial conditions with the proposed control scheme called sliding mode control (SMC) based on the time-delay chaotic systems. In comparison, the fractional-order Lyapunov direct method (FLDM) is proposed and is implemented to SMC to maintain the systems' sturdiness and assure the global convergence of the error dynamics. An extensive literature survey has been conducted, and we found that many researchers focus only on fractional order of neural networks (FNNs) without delay in different systems. Furthermore, the proposed method has been tested with different multi-fractional orders and time-delay values to find the most stable MFNNMD. Finally, numerical simulations are presented by taking two MFNNMDs as an example to confirm the effectiveness of our control scheme.

1. Introduction

Although the concept and the knowledge of fractional-order calculus have existed since L'Hôpital's and Leibniz's contribution in 1695s [1, 2], its applications to the real world of mathematics, physics engineering, and biology are only of interest recently [3, 4]. As a result, it has captured the attention of physicists and engineers over the last decade and has been a new trend up until this point. In addition, due to its universal application in different fields, such as brain networks, fractional-order dynamical systems have generated significant study attention. As opposed to integer-order systems, fractional-order systems exhibit long-term memory effects, making them ideal for representing varied materials and processing more precisely [5]. Fractional-order modeling has the capacity to explain real-world phenomena more realistically and precisely compared to the traditional integer-order calculus [6–8], making it particularly well adapted to study nonlinear systems, predominantly in biology and physics.

The fractional-order chaotic system synchronization has recently garnered attention because of its capability of application in a diversity of physics and engineering science fields, including encryption and secure communication. As a result, there is considerable interest in properly synchronizing two chaotic systems with fractional order. Synchronization behavior is a fundamental natural phenomenon that frequently occurs in both the natural world and engineering. Chaos synchronization has garnered substantial interest and research over the last few years because of its tenacity in numerous fields, including secure communication, physical science, chemical reactors, and information processing. Numerous intriguing discoveries have been found thus far on chaotic synchronization [9–13]. However, the widely held research is based on synchronization asymptotically. Alternatively, we can say that synchronization of chaos can occur individually when the time approaches infinity.

As we all know, it is more useful in reality for chaotic systems to be synchronized within finite time preferably

compared to infinite time. As a result, much study has been conducted on fixed-time synchronization [14–17]. Fixed-time synchronization denotes the possibility of achieving chaos synchronization within a finite time window for any initial value of the examined system. In comparison to synchronization asymptotically, fixed-time synchronization has several advantages, including a faster convergence rate and enhanced anti-interference capacity. The error system must be stable for a defined period to maintain chaos synchronization within a fixed time. Even though certain conclusions have been recommended in the literature, the study of chaotic systems' fixed temporal stability is still in its infancy. Thus, it is critical to continue developing some innovative and effective fixed-time stability criteria.

Following Pecora and Carroll's first work on chaotic synchronization [18], synchronization of neural networks (NNs) and complex networks has become an important topic. Due to the enormous advantages of controlling a problem and addressing complex nonlinear system analysis, NN-based modeling has been an active study area in recent years. Besides, there are some disadvantages in synchronization among NN systems, and the results of numerous control methods have been proven to deal with drawbacks, including adaptive [19], generalized projective [20], linear feedback [21], and SMC [22]. The adaptive SMC approach is an efficient technique for synchronizing chaotic systems with a fractional order among the strategies outlined above. The essential characteristics of this technique are its rapid reaction, resistance to perturbations, sensitivity to parameter disturbances, good momentary performance, and effortlessness of application in real-world applications. We discovered that projective synchronization could achieve remarkable performance in secure communication due to its proportional function.

According to prior studies, synchronization of identical or nonidentical FNNs occurs without delay [19, 22–24]. Indeed, there is always some noise and disturbances that might impair performance and impair the synchronization's output. However, from the standpoint of practical engineering, the work presented in the preceding publications is insufficient since they ignore the influence of time delays on the system, which is another crucial component contributing to the loss of system stability. Time delays are inevitable as a result of information's finite propagation velocity [25, 26], the potential of feedback loops, and the finite switching durations. In the real world, many channels of data alternation, multiple switching mechanisms, and two or more feedback systems may exist [27]. Conversely, multi-time delay systems are frequently more accurate representations of interacting complex systems than single-time-delay systems.

FNNs with multi-time-delay synchronization are extremely important to study. In the later years, delayed differential equations have been broadly studied as in [28, 29]. Recently, chaotic systems have been developed with temporal and time-varying delays; for example, see [30–33]. In addition, the first study on the significance of time delay on chaotic behavior was in [34] based on the previous literature. Nevertheless, most of these papers concern about ordinary differential equations or integer orders, and there are preliminary results concerning chaos synchronization of FNNs with multi-time-delay systems. Numerous researchers have attempted to employ the FNNs with multi-time-delay systems to research secure communication, and they have come up with some exciting results in [35–38].

There are two widely used techniques for dealing with the degradation of system stability caused by time delays: Lyapunov–Razumikhin functions (LRFs) and Lyapunov–Krasovskii functions (LKFs) [37, 38]. In addition, the separation technique is frequently used to decompose unknown time-delayed functions into numerous continuous functions [39]. In [37], a Lyapunov–Razumikhin approach was created, and theoretical results established that systems with varying time delays might be stable in infinite time.

Nonetheless, to the best of the authors' understanding, no researcher has yet examined the theoretical investigation of MFNNMD. Indeed, this fascinating subject remains an open challenge, which prompted our investigation. As a result, this study analyses the dynamic properties of MFNNMD systems. We introduced the global Mittag–Leffler MFNNMD model of projective synchronization in our work and designed a new multidelay SMC controller. Following that, a new extended concept for cryptography and safe communication is introduced for further research. The following are the primary aspects of this article's significant contributions:

(1) For the first time, MFNNMD is investigated.

(2) We are constructing appropriate proposed multi-time-delay SMC controller and FLDM of the error system for global Mittag–Leffler synchronization of MFNNMD to maintain their stability and ensure global convergence of the error dynamics.

(3) To determine the practical significance of the theoretical outcomes, a numerical example is provided with simulations. In addition, other examples are included in the table.

(4) Finally, we hope that our research will provide significant results to the real world, resulting in increased security in secure communication networks.

Our proposed technique is particularly well-suited for secure communication. The transmission signal is transferred from the transmitter to the recipient by a chaotic motion across an analogue network in a normal chaotic synchronization communication technique. Numerous methods for masking the data in transmission signals using chaotic signals have been developed, including chaotic-switching and chaotic-modulation approaches. However, it has been demonstrated that the majority of these schemes are insecure as the encrypted message signal may be hacked or extracted from the transmitted chaotic signal using several unmasking techniques. By employing our proposed synchronization strategy to broadcast the signal, the transmitted signal can be added to MFNNMD. We believe that our proposed method can help chaotic communication become more secure.

The following is the organization of this article: Section 2 contains an explanation of the system and some relevant prerequisites. In Section 3, we examine the synchronization of chaotic systems with MFNNMD. In Section 4, we carry out numerical simulations to confirm and validate our theoretical results' practicality and discuss the implications of varying fractional orders and time delays on synchronization. Finally, in Section 5, we conclude the article.

2. Preliminaries and Description of the Model

Two definitions of the most conventional fractional-order calculus derivatives used are mentioned in the literature: the Caputo and the Riemann–Liouville. Then, the Caputo derivative is implemented in this work because its initial conditions may indeed be described in terms of integer-order derivatives, which is more practical in practice.

Definition 1 (see [40]). For the $u(t)$ function, the fractional derivative of Caputo order α is described as

$$\mathscr{D}^{\alpha}u(t) = \frac{1}{\Gamma(q-\alpha)}\int_0^t (t-\tau)^{q-\alpha-1}u^{(q)}(\tau)\mathrm{d}\tau, \tag{1}$$

where $t \geq t_0$, q is the integer, $q-1 < \alpha < q$, $\Gamma(\cdot)$ is a Gamma function, and $\Gamma(p) = \int_0^{\infty} t^{p-1}e^{-t}\mathrm{d}t$.

In this research, we study the following NNs, which we designate to as MFNNMD, where the DS is denoted as

$$\begin{aligned}\mathscr{D}^{\alpha_i}\mathscr{X}_i(t) = &-c_i\mathscr{X}_i(t) + \sum_{j=1}^{x} a_{ij}f_j\left(\mathscr{X}_j(t)\right)\\ &+ \sum_{j=1}^{x} g_{ij}f_j\left(\mathscr{X}_j\left(t-\tau_j\right)\right) + \varphi_i,\end{aligned} \tag{2}$$

where $0 < \alpha_i < 1, i, j = 1, 2, \ldots, x$, x represents the unit number in a MFNNMD, $\mathscr{X}_i(t)$ signifies the i-th neuron's pseudo-state variable of the DS, and $c_i > 0$ is the ith unit parameters. The external input of the ith unit is φ_i, a_{ij} and g_{ij} denote the relation of the unit jth with the i th at time t and $t-\tau_j$, respectively, $\tau_j > 0$ is the delayed transmission, and $f_j(\mathscr{X}_j(t))$ and $f_j(\mathscr{X}_j(t-\tau_J))$ represent the j-th unit activation function output at time t and $t-\tau_j$, respectively.

Also, the vector form

$$\mathscr{D}^{\alpha_i}\mathscr{X}(t) = -\mathrm{C}\mathrm{X}(t) + Af_{\mathrm{c}}(\mathscr{X}(t)) + Gf_c\left(\mathscr{X}\left(t-\tau_j\right)\right) + \varphi. \tag{3}$$

The corresponding RS of MFNNMD is denoted as

$$\begin{aligned}\mathscr{D}^{\alpha_i}y_i(t) = &-d_iy_i(t) + \sum_{j=1}^{x} b_{ij}g_j\left(y_j(t)\right) + \sum_{j=1}^{x} h_{ij}g_j\left(y_j\left(t-\tau_j\right)\right)\\ &+ \mu_i + \vartheta_i(t),\end{aligned} \tag{4}$$

where $0 < \alpha_i < 1, i, j = 1, 2, \ldots, x$, x represents the unit number in a MFNNMD, $y_i(t)$ represents the ith unit's pseudo-state variable of the RS, and $d_i > 0$ is the ith neuron's parameters. μ_i represents the external input of the ith unit, b_{ij} and h_{ij} denote the relation of the unit jth with the ith at time t and $t-\tau_j$, respectively, $\tau_j > 0$ is the delayed transmission, and $g_j(y_j(t))$ and $g_j(y_j(t-\tau))$ denote the jth unit activation function output at time t and $t-\tau_j$, respectively. However, $\vartheta_i(t)$ is an appropriate controller. For simplifications, in the next part, definition, lemmas, and theorems are given.

Definition 2. By establishing the one-parameter Mittag–Leffler function by setting $\alpha > 0$ and $u \in C$, then

$$E_{\alpha}(u) = \sum_{k=0}^{\infty}\frac{u^k}{\Gamma(k\alpha+1)}. \tag{5}$$

and by establishing the two-parameter Mittag–Leffler function by setting $\alpha > 0, \beta > 0$, and $u \in C$, then

$$E_{\alpha,\beta}(u) = \sum_{k=0}^{\infty}\frac{u^k}{\Gamma(k\alpha+\beta)}. \tag{6}$$

According to Definition 2, it is not difficult to see $E_{\alpha}(u) = E_{\alpha,1}(u)$ and $E_{1,1}(u) = e^u$.

Definition 3 (see [19]). Suppose there is a constant of nonzero, ρ, such that sufficiently for every result of $\mathscr{X}(t)$ and $Y(t)$ for systems (2) and (4) using distinct initial condition, you may obtain

$$\lim_{t\longrightarrow+\infty}\Upsilon(t) - \rho\mathscr{X}(t) = 0. \tag{7}$$

Therefore, DS (2) and RS (4) can accomplish globally projective synchronization asymptotically, i representing the vector's Euclidean norm.

Lemma 1 (see [41]). *Assume $\mathscr{X}(t) \in R$ is a continuous function of differentiable vector value. Hence, for whichever time prompt $\geq t_0$, we get the following:*

$$D^{\alpha}\mathscr{X}^T(t)\mathscr{X}(t) \leq 2\mathscr{X}^T(t)D^{\alpha}\mathscr{X}(t), \tag{8}$$

where $0 < \alpha < 1$.

3. Controller Design and Stability Analysis

Two identical MFNNMD synchronization conditions are achieved in this section by proposing an appropriate controller. Define the errors of synchronization as $(t) = \Upsilon_i(t) - \rho\mathscr{X}_i(t)$ $(i = 1, 2, \ldots, x)$. Based on DS (2) and RS (4), the control function $\vartheta_i(t)$ $(i = 1, 2, \ldots, x)$ can be designated as follows:

$$\vartheta_i(t) = -\left[c_i + \left(\Pi_{jl}\right)_{x\times m}\cdot(\omega_{li})_{m\times x} - d_i\right]\mathfrak{E}_j(t) - \left[\left(\Pi_{jl}\right)_{x\times m}\cdot(\varepsilon_{li})_{m\times x}\right]\mathfrak{E}_j\left(t-\tau_j\right) - \rho(c_i-d_i)\mathcal{X}_j(t) - \sum_{j=1}^{\aleph} b_{ij}g_j\left[\rho\mathcal{X}_j(t)\right] - \sum_{j=1}^{\aleph} h_{ij}g_j\left[\rho\mathcal{X}_j\left(t-\tau_j\right)\right] + \rho\sum_{j=1}^{\aleph} a_{ij}f_j\left[\mathcal{X}_j(t)\right] + \rho\sum_{j=1}^{\aleph} g_{ij}f_j\left[\mathcal{X}_j(t)\right] - \rho\varphi_i + \mu_i, \tag{9}$$

where $i, j, \aleph, m = 1, 2, \ldots, \aleph$ and ρ is the projective coefficient. From (2), (4), and (9), you can get the $\mathscr{D}^{\alpha}\mathfrak{E}(t)$ error system as follows:

$$\mathscr{D}^{\alpha_i}\mathfrak{E}(t) = d_ie_i(t) + \sum_{j=1}^{x} b_{ij}\left[g_j\left(\Upsilon_j(t)\right) - g_j\left(\rho\mathcal{X}_j(t)\right)\right] + \sum_{j=1}^{x} h_{ij}\left[g_j\left(\Upsilon_j\left(t-\tau_j\right)\right) - g_j\left(\rho\mathcal{X}_j\left(t-\tau_j\right)\right)\right] + \rho(c_i-d_i)\mathcal{X}_j(t) + \sum_{j=1}^{x} b_{ij}\left[g_j\left(\mathcal{X}_j(t)\right)\right] + \sum_{j=1}^{x} h_{ij}\left[g_j\left(\rho\mathcal{X}_j\left(t-\tau_j\right)\right)\right] - \rho\sum_{j=1}^{x} a_{ij}\left[f_j\left(\mathcal{X}_j(t)\right)\right] - \rho\sum_{j=1}^{x} g_{ij}\left[f_j\left(\mathcal{X}_j\left(t-\tau_j\right)\right)\right] - \rho\varphi_i + \mu_i + \vartheta_i(t). \tag{10}$$

Now, (9) and (10) are combined together and the error system of delayed sliding mode dynamics (DDMDEs), $\mathscr{D}^{\alpha}\mathfrak{E}(t)$, can be defined by

$$\mathscr{D}^{\alpha_i}\mathfrak{E}(t) = -\left[c_i + \left(\Pi_{jl}\right)_{x\times m}\cdot(\omega_{li})_{m\times x}\right]\mathfrak{E}_i(t) - \left[\left(\Pi_{jl}\right)_{x\times m}\cdot(\varepsilon_{li})_{m\times x}\right]\mathfrak{E}_j\left(t-\tau_j\right) + \sum_{j=1}^{x} b_{ij}\left[g_j\left(\Upsilon_j(t)\right) - g_j\left(\rho\mathcal{X}_j(t)\right)\right] + \sum_{j=1}^{x} h_{ij}\left[g_j\left(\Upsilon_j\left(t-\tau_j\right)\right) - g_j\left(\rho\mathcal{X}_j\left(t-\tau_j\right)\right)\right]. \tag{11}$$

Then, it follows from (11) that

$$\mathscr{D}^{\alpha_i}\mathfrak{E}(t) = -c_ie_i(t) - \left[\sum_{j=1}^{x}\sum_{l=1}^{m}\left(\Pi_{jl}\right)(\omega_{li})\right]\mathfrak{E}_i(t) - \left[\sum_{j=1}^{x}\sum_{l=1}^{m}\left(\Pi_{jl}\right)(\varepsilon_{li})\right]\mathfrak{E}_j\left(t-\tau_j\right) + \sum_{j=1}^{x} b_{ij}\left[g_j\left(\Upsilon_j(t)\right) - g_j\left(\rho\mathcal{X}_j(t)\right)\right] + \sum_{j=1}^{x} h_{ij}\left[g_j\left(\Upsilon_j\left(t-\tau_j\right)\right) - g_j\left(\rho\mathcal{X}_j\left(t-\tau_j\right)\right)\right]. \tag{12}$$

To investigate the stability of DDMDEs (11) in this paper, Theorem 1 is stated.

Theorem 1 (see [42]). *Assume that condition (H) is met and there are positive constants called m_i and l_i in such a way that $m_i = \max\{|m_i^-|, |m_i^+|\}$ and $l_i = \max\{|l_i^-|, |l_i^+|\}$ and constant matrices that $(\Pi_{jl})_{\aleph\times i}$, $(\omega_{li})_{m\times\aleph}$, $(\varepsilon_{li})_{i\times\aleph}$, and*

$$\begin{cases} \Psi_1 := \min\limits_{1\le i\le x}\left[c_i - \sum\limits_{j=1}^{x}\left[\sum\limits_{l=1}^{m}\left|\left(\Pi_{jl}\right)(\omega_{li})\right|\right] - \sum\limits_{j=1}^{x}\left|b_{ji}\right|m_i\right] > 0, \\ \Psi_2 := \max\limits_{1\le i\le x}\left[\sum\limits_{j=1}^{x}\left[\sum\limits_{l=1}^{m}\left|\left(\Pi_{jl}\right)(\varepsilon_{li})\right|\right] + \sum\limits_{j=1}^{x}\left|h_{ji}\right|l_i\right] > 0, \\ \Psi_1 - \Psi_2 > 0. \end{cases} \tag{13}$$

Then, equation (11) is stable.

Proof of Theorem 1. According to (H) and Theorem 1, we have

$$m_j^- \le \frac{g_j[\Upsilon_j(t)] - g_j[\rho\mathscr{X}_j(t)]}{(\Upsilon_j(t)) - (\rho\mathscr{X}_j(t))} \le m_j^+, \tag{14}$$

$$l_j^- \le \frac{g_j[\Upsilon_j(t-\tau_j)] - g_j[\rho\mathscr{X}_j(t-\tau_j)]}{(\Upsilon_j(t-\tau_j)) - (\rho\mathscr{X}_j(t-\tau_j))} \le l_j^+. \tag{15}$$

Next, we obtain that

$$\begin{cases} |g_j[\Upsilon_j(t)] - g_j[\rho\mathscr{X}_j(t)]| \le m_j|(\Upsilon_j(t)) - (\rho\mathscr{X}_j(t))|, \\ |g_j[\Upsilon_j(t-\tau_j)] - g_j[\rho\mathscr{X}_j(t-\tau_j)]| \le l_j|(\Upsilon_j(t-\tau_j)) - (\rho\mathscr{X}_j(t-\tau_j))|. \end{cases} \tag{16}$$

Generate the following function of Lyapunov:

$$V[\mathfrak{E}(t)] = \sum_{i=1}^{x} |\mathfrak{E}_i(t)|. \tag{17}$$

As a result of Lemma 1, by applying the Caputo derivative's upper right $\mathscr{D}_+^{\alpha}[\mathfrak{E}(t)]$ along the trajectories, equation (17) can be obtained as follows.

We defined the Lyapunov function by

$$\begin{aligned}
\mathscr{D}_+^{\alpha_i} V[\mathfrak{E}_i(t)] &= \sum_{i=1}^{x} \mathscr{D}_+^{\alpha_i} |\mathfrak{E}_i(t)| \le -\sum_{i=1}^{x} \operatorname{sgn}[\mathfrak{E}_i(t)] D_+^{\alpha} \mathfrak{E}_i(t) \\
&= -\sum_{i=1}^{x} \operatorname{sgn}[\mathfrak{E}_i(t)] \left[\left[c_i + \sum_{j=1}^{x} \left[\sum_{l=1}^{m} (\Pi_{jl})(\omega_{li}) \right] \right] \mathfrak{E}_j(t) + \left[\sum_{j=1}^{x} \left[\sum_{l=1}^{m} (\Pi_{jl})(\varepsilon_{li}) \right] \right] \mathfrak{E}_j(t-\tau_j) + \sum_{j=1}^{x} b_{ij} [g_j(\Upsilon_j(t)) - g_j(\rho\mathscr{X}_j(t))] \right. \\
&\quad \left. + \sum_{j=1}^{x} h_{ij} [g_j(\Upsilon_j(t-\tau_j)) - g_j(\rho\mathscr{X}_j(t-\tau))] \right] \le -\sum_{i=1}^{x} c_i |\mathfrak{E}_i(t)| + \sum_{i=1}^{x} \left[\sum_{j=1}^{x} \left[\sum_{l=1}^{m} |(\Pi_{jl})(\omega_{li})| \right] |\mathfrak{E}_j(t)| \right] + \sum_{i=1}^{x} \left[\sum_{j=1}^{x} \left[\sum_{l=1}^{m} |(\Pi_{jl})(\varepsilon_{li})| |\mathfrak{E}_j(t-\tau_j)| \right] \right] \\
&\quad + \sum_{i=1}^{x} \left[\sum_{j=1}^{x} |b_{ij}| m_j |(\Upsilon_j(t)) - (\rho X_j(t))| \right] + \sum_{i=1}^{x} \left[\sum_{j=1}^{x} |h_{ij}| l_j |(\Upsilon_j(t-\tau_j)) - (\rho\mathscr{X}_j(t-\tau_j))| \right], \\
&= -\sum_{i=1}^{x} c_i |\mathfrak{E}_i(t)| + \sum_{i=1}^{x} \left[\sum_{j=1}^{x} \left[\sum_{l=1}^{m} |(\Pi_{jl})(\omega_{li})| \right] |\mathfrak{E}_i(t)| + \sum_{i=1}^{x} \left[\sum_{j=1}^{x} \left[\sum_{l=1}^{m} |(\Pi_{jl})(\varepsilon_{li})| \right] |\mathfrak{E}_j(t-\tau_j)| + \sum_{i=1}^{x} \left[\sum_{j=1}^{x} |b_{ij}| m_j |(\Upsilon_j(t)) - (\rho\mathscr{X}_j(t))| \right] \right. \\
&\quad \left. + \sum_{i=1}^{x} \left[\sum_{j=1}^{x} |h_{ij}| l_j |(\Upsilon_j(t-\tau_j)) - (\rho\mathscr{X}_j(t-\tau_j))| \right], \right. \\
&= -\sum_{i=1}^{x} \left[c_i - \left[\sum_{j=1}^{x} \left[\sum_{l=1}^{m} |(\Pi_{jl})(\omega_{li})| \right] \right] - \left[\sum_{j=1}^{x} |b_{ij}| m_j |(\Upsilon_j(t)) - (\rho\mathscr{X}_j(t))| \right] \right] |\mathfrak{E}_i(t)| + \left[\sum_{i=1}^{x} \left[\sum_{j=1}^{x} \left[\sum_{l=1}^{m} |(\Pi_{jl})(\varepsilon_{li})| \right] \right] \right. \\
&\quad \left. + \sum_{i=1}^{x} \left[\sum_{j=1}^{x} |h_{ij}| l_j |(\Upsilon_j(t-\tau_j)) - (\rho X_j(t-\tau_j))| \right] \right] |\mathfrak{E}_j(t-\tau_j)|, \\
&= \max_{1\le i\le x} \left[\sum_{j=1}^{x} \left[\sum_{l=1}^{m} |(\Pi_{jl})(\varepsilon_{li})| \right] + \sum_{j=1}^{x} |h_{ji}| l_i \right] |\mathfrak{E}_j(t-\tau_j)| - \min_{1\le i\le x} \left[c_i - \sum_{j=1}^{x} \left[\sum_{l=1}^{m} |(\Pi_{jl})(\omega_{li})| \right] - \sum_{j=1}^{x} |b_{ji}| m_i \right] |\mathfrak{E}_i(t)| \le \Psi_1 V(\mathfrak{E}_i(t)) + \Psi_2 \sup_{t-\tau_j\le u\le t} V(\mathfrak{E}_i(u)).
\end{aligned} \tag{18}$$

Note that

$$\sup_{t-\tau_j \le u \le t} V(\mathfrak{E}_i(u)) \le V(\mathfrak{E}_i(t)). \tag{19}$$

Then, assuming that there is a constant Δ greater than zero in conjunction with (18) and (19) and Theorem 1, one has

$$\begin{cases} \mathscr{D}_+^{\alpha_i} V(\mathfrak{E}_i(t)) \le -(\Psi_1 - \Psi_2) V(\mathfrak{E}_i(t)), \\ \Psi_1 - \Psi_2 \ge \Delta. \end{cases} \tag{20}$$

We construct that (18) as

$$\mathscr{D}_+^{\alpha_i} V(\mathfrak{E}_i(t)) \le \Delta V(\mathfrak{E}_i(t)), \tag{21}$$

so

$$\begin{aligned}
\|\mathfrak{E}_i(t)\| &= \|(\Upsilon_j(t)) - (\rho\mathscr{X}_j(t))\| \\
&= \sum_{i=1}^{\aleph} \|(\Upsilon_j(t)) - (\rho\mathscr{X}_j(t))\|.
\end{aligned} \tag{22}$$

Finally, we can conclude that DDMDEs (9) are stable as $\mathfrak{E}_i(t) \longrightarrow 0$ as t approaches infinity.

This completes the proof. □

Remark 1. When = 1, projective synchronization is standardized by multiple time delays for the complete synchronization of MFNNMD.

Remark 2. When = −1, the projective synchronization is standardized to the complete globally antisynchronization of MFNNMD with multiple time delays.

Remark 3. No study on the topic of MFNNMD chaotic synchronization has been published so far. As a result of addressing these inadequacies, we developed for the first time new necessary conditions for ensuring the chaos synchronization of MFNNMD systems is archived. As a result, the paper's primary findings are significantly new compared to those found in the prior literature.

4. Numerical Experiments

The following example demonstrates that the control method proposed in this study is capable of adequately managing the time-delay system's stability while guaranteeing that all state variables remain within the specified ranges. Here, two types of experiments of time delay with alpha are introduced.

4.1. Projective Chaos Synchronization of MFNNMD Systems

4.1.1. Experiment A: Synchronization of MFNNMD Systems with Fixed Time Delay, $\tau = 0.11$. Assuming that two MFNNMD systems are synchronized with each other, define the drive system as

$$\begin{aligned}
\mathscr{D}^{\alpha_1}\mathscr{X}_1(t) &= -c_1\mathscr{X}_1 + a_{11}f_1(\mathscr{X}_1(t)) + a_{12}f_2(\mathscr{X}_2(t)) + a_{13}f_3(\mathscr{X}_3(t)) + a_{14}f_4(\mathscr{X}_4(t)) + g_{11}f_1(\mathscr{X}_1(t-\tau_1))\\
&\quad + g_{12}f_2(\mathscr{X}_2(t-\tau_1)) + g_{13}f_3(\mathscr{X}_3(t-\tau_1)) + g_{14}f_4(\mathscr{X}_4(t-\tau_1)) + \varphi_1,\\
\mathscr{D}^{\alpha_2}\mathscr{X}_2(t) &= -c_2\mathscr{X}_2 + a_{21}f_1(\mathscr{X}_2(t)) + a_{22}f_2(\mathscr{X}_2(t)) + a_{23}f_3(\mathscr{X}_3(t)) + a_{24}f_4(\mathscr{X}_4(t)) + g_{21}f_1(\mathscr{X}_1(t-\tau_2))\\
&\quad + g_{22}f_2(\mathscr{X}_2(t-\tau_2)) + g_{23}f_3(\mathscr{X}_3(t-\tau_2)) + g_{24}f_4(\mathscr{X}_4(t-\tau_2)) + \varphi_2,\\
\mathscr{D}^{\alpha_3}\mathscr{X}_3(t) &= -c_3\mathscr{X}_3 + a_{31}f_1(\mathscr{X}_1(t)) + a_{32}f_2(\mathscr{X}_2(t)) + a_{33}f_3(\mathscr{X}_3(t)) + a_{34}f_4(\mathscr{X}_4(t)) + g_{31}f_1(\mathscr{X}_1(t-\tau_3))\\
&\quad + g_{32}f_2(\mathscr{X}_2(t-\tau_3)) + g_{33}f_3(\mathscr{X}_3(t-\tau_3)) + g_{34}f_4(\mathscr{X}_4(t-\tau_3)) + \varphi_3,\\
\mathscr{D}^{\alpha_4}\mathscr{X}_4(t) &= -c_4\mathscr{X}_4 + a_{41}f_1(\mathscr{X}_1(t)) + a_{42}f_2(\mathscr{X}_2(t)) + a_{43}f_3(\mathscr{X}_3(t)) + a_{44}f_4(\mathscr{X}_4(t)) + g_{41}f_1(\mathscr{X}_1(t-\tau_4))\\
&\quad + g_{42}f_2(\mathscr{X}_2(t-\tau_4)) + g_{43}f_3(\mathscr{X}_3(t-\tau_4)) + g_{44}f_4(\mathscr{X}_4(t-\tau_4)) + \varphi_4.
\end{aligned} \tag{23}$$

And, define the response system as

$$\begin{aligned}
\mathscr{D}^{\alpha_5}\Upsilon_1(t) &= -d_1\Upsilon_1 + b_{11}f_1(\Upsilon_1(t)) + b_{12}f_2(\Upsilon_2(t)) + b_{13}f_3(\Upsilon_3(t)) + a_{14}f_4(\Upsilon_4(t)) + h_{11}f_1(\Upsilon_1(t-\tau_1))\\
&\quad + h_{12}f_2(\Upsilon_2(t-\tau_5)) + h_{13}f_3(\Upsilon_3(t-\tau_5)) + h_{14}f_4(\Upsilon_4(t-\tau_5)) + \mu_1 + \vartheta_1(t),\\
\mathscr{D}^{\alpha_6}\Upsilon_2(t) &= -d_2\Upsilon_2 + b_{21}f_1(\Upsilon_2(t)) + b_{22}f_2(\Upsilon_2(t)) + b_{23}f_3(\Upsilon_3(t)) + b_{24}f_4(\Upsilon_4(t)) + h_{21}f_1(\Upsilon_1(t-\tau_6))\\
&\quad + h_{22}f_2(\Upsilon_2(t-\tau_6)) + h_{23}f_3(\Upsilon_3(t-\tau_6)) + h_{24}f_4(\Upsilon_4(t-\tau_6)) + \mu_2 + \vartheta_2(t),\\
\mathscr{D}^{\alpha_7}\Upsilon_3(t) &= -d_3\Upsilon_3 + b_{31}f_1(\Upsilon_1(t)) + b_{32}f_2(\Upsilon_2(t)) + b_{33}f_3(\Upsilon_3(t)) + b_{34}f_4(\Upsilon_4(t)) + h_{31}f_1(\Upsilon_1(t-\tau_7))\\
&\quad + h_{32}f_2(\Upsilon_2(t-\tau_7)) + h_{33}f_3(\Upsilon_3(t-\tau_7)) + h_{34}f_4(\Upsilon_4(t-\tau_7)) + \mu_3 + \vartheta_3(t),\\
\mathscr{D}^{\alpha_8}\Upsilon_4(t) &= -d_4\Upsilon_4 + b_{41}f_1(\Upsilon_1(t)) + b_{42}f_2(\Upsilon_2(t)) + b_{43}f_3(\Upsilon_3(t)) + b_{44}f_4(\Upsilon_4(t)) + h_{41}f_1(\Upsilon_1(t-\tau_8))\\
&\quad + h_{42}f_2(\Upsilon_2(t-\tau_8)) + h_{43}f_3(\Upsilon_3(t-\tau_8)) + h_{44}f_4(\Upsilon_4(t-\tau_8)) + \mu_4 + \vartheta_4(t),
\end{aligned} \tag{24}$$

with the following parameters: $\alpha_1 = 0.985$, $\alpha_2 = 0.980$, $\alpha_3 = 0.975$, $\alpha_4 = 0.970$, $\alpha_5 = 0.965$, $\alpha_6 = 0.960$, $\alpha_7 = 0.955$, $\alpha_8 = 0.950$, $c_1 = c_4 = -9.5$, $c_2 = -10.5$, $c_3 = -3.7$, $a_{11} = 2.0$, $a_{12} = 0.5$, $a_{13} = 5.5$, $a_{14} = 2$, $a_{21} = 0.5$, $a_{22} = 0.5$, $a_{23} = 5.1$, $a_{24} = 0.5$, $a_{31} = 0.5$, $a_{32} = 1.0$, $a_{33} = -5.5$, $a_{34} = 5.1$, $a_{41} = 0.5$, $a_{42} = 1.0$, $a_{43} = -9.5$, $a_{44} = 0.5$ $g_{11} = 7$, $g_{12} = 7$, $g_{13} = 4.1$, $g_{14} = 7$, $g_{21} = 1$, $g_{22} = 1$, $g_{23} = 2.5$, $g_{24} = 1$, $g_{31} = 0.1$, $g_{32} = -10.1$, $g_{33} = 4.5$, $g_{34} = 0.1$, $g_{41} = 7$, $g_{42} = 7$, $g_{43} = 4.1$, $g_{44} = 7$, $d_1 = d_4 = -1$, $d_2 = -3$, $d_3 = -7.7$, $b_{11} = 0.01$, $b_{12} = 0.3$, $b_{13} = 7.5$, $b_{14} = 0.01$, $b_{21} = 0.01$, $b_{22} = 7.5$, $b_{23} = 0.01$, $b_{24} = 0.01$, $b_{31} = 0.01$, $b_{32} = 3$, $b_{33} = -5.5$, $b_{34} = -5.5$, $b_{41} = 0.01$, $b_{42} = 3$, $b_{43} = 3$, $b_{44} = -5.5$, $h_{11} = 0.3$, $h_{12} = 5.5$, $h_{13} = 5.5$, $h_{14} = 0.3$, $h_{21} = 0.5$, $h_{22} = 7.5$, $h_{23} = 0.01$, $h_{24} = 0.5$, $h_{31} = 0.1$, $h_{32} = -1.5$, $h_{33} = 1.5$, $h_{34} = 0.1$, $h_{41} = 0.1$, $h_{42} = 5.5$, $h_{43} = 5.5$, $h_{44} = 0.1$, $f_1(.) = f_2(.) = f_3(.) = f_4(.) = tanh(\mathscr{X})$, $\varphi_1 = \varphi_2 = \varphi_3 = \varphi_4 = 0$,

$\mu_1 = \mu_2 = \mu_3 = \mu_4 = 0$, and $\vartheta_1(t) = \vartheta_2(t) = \vartheta_3(t) = \vartheta_4(t) = 1$.

With the above initial values, parameters, and controller gain, we solve the numerical solutions of DS (21), RS (22), and error system (11) using MATLAB tools. Furthermore, we use the step-by-step iteration method to solve the fractional differential-difference equations part. Then, they are illustrated in Figures 1–4.

A graphical representation in phase portrait of the consequences of MFNNMD synchronization is shown in Figure 1 using $\mathcal{X}$ and Υ, as the dependent variables. At the same time, t is an independent variable function. Figure 2 shows a phase portrait of synchronization of MFNNMD, when $\tau = 0.11$ and alpha = [0.995, 0.990, 0.985, 0.980, 0.975, 0.970, 0.965, 0.960]. Chaos synchronization of the MFNNMD system with and without the controller activation is shown in Figure 3. As illustrated in Figure 4, the dynamic error is unable to converge to zero when the controller is not engaged. However, when the controller is activated, the dynamic error does converge to zero in a limited time. As illustrated in Figure 4, master-slave systems (21) and (22) exhibit global Mittag–Leffler asymptotic synchronization, confirming the validity and effectiveness of the criteria specified in Theorem 1.

4.1.2. Experiment B: Synchronization of Two MFNNMD Systems with Multi-Time Delay, $\tau = [0.10, 0.11, 0.12, 0.13, 0.14, 0.15, 0.16, 0.17]$. The numerical experiment of synchronization of two MFNNMD systems is demonstrated in this section. In this experiment, we consider system changes at different fractional orders and different time delays. The same systems of DS (21) and (22) are used. Figure 5 shows that the systems have chaotic characteristics, while Figure 6 shows a phase portrait of synchronization of MFNNMD, when $\tau = [0.10, 0.11, 0.12, 0.13, 0.14, 0.15, 0.16, 0.17]$ and alpha = [0.995, 0.990, 0.985, 0.980, 0.975, 0.970, 0.965, 0.960]. The synchronization of the MFNNMD system with and without the controller activation is shown in Figure 7. Furthermore, for the error dynamics in Figure 8, we can see that the dynamic error is unable to converge to zero when the controller is not engaged. However, when the controller is activated, the dynamic error does converge to zero in a limited time.

4.2. Effects on Chaos Synchronization of α-Order and τ-Time Delay. According to the literature, α-order affects the performance of fractional-order chaotic dynamical systems. As previously demonstrated, time delay affects the performance of chaotic dynamical systems. In the actual world, time delays are pervasive and unavoidable. The time-delay dynamic system exhibits complicated dynamic characteristics that are frequently utilized to illustrate time-delayed engineering issues. In this paper, two NN chaotic systems that act as DS and RS are used to examine the dynamic performance from the effect of multi-fractional order and multi-time delay on nonlinear dynamic systems. Furthermore, the capability of the SMC design in this research is studied to prove that it can control the MFNNMD system.

From Figure 2, we consider system changes at different fractional orders with the alpha = [0.995, 0.990, 0.985, 0.980, 0.975, 0.970, 0.965, 0.960] while fixing delay $\tau = 0.11$. We can learn from Figure 2 that the system becomes chaotic and the system trajectory becomes periodic. The system continues to be chaotic as different values of alpha are applied, for example, alpha = [0.895, 0.890, 0.885, 0.880, 0.875, 0.870, 0.865, 0.860] and alpha = [0.795, 0.790, 0.785, 0.780, 0.775, 0.770, 0.765, 0.760]. From Figures 9(a) and 9(b), if we continue decreasing the value of fractional orders, we can see that the systems slowly produce the intermittent chaos phenomenon. Finally, when the value of alpha = [0.695, 0.690, 0.685, 0.680, 0.675, 0.670, 0.665, 0.660], as shown in Figure 9(c), the system will be unstable and lose its chaotic characteristic.

This section addresses the effects of altering the α-order and τ-time delay on chaotic synchronization. We summarised some observations about the error functions for various values of α at specified time values in Table 1. As shown in Table 1, the synchronization error reduces as the order of α is raised. In other words, the synchronization process begins earlier with a greater value of α.

Based on Experiment A, Table 1 contains some results on the dynamic error for different order values in system (21) and system (22). Here, trials are conducted with a fixed delay value of $\tau = 0.11$. It is evident that as the order drops, the synchronization error increases first and subsequently reduces, which is not the case in [43]. Simultaneously, we sum up some data related to the dynamic error for a different combination of fractional orders with the fixed time delay in systems (21) and (22). As seen in Table 1, the dynamic errors $e_1(t), e_2(t), e_3(t)$, and $e_4(t)$ converge to zero as time increases. Precisely, the error function reduces first, then increases, and eventually decreases over the time points for all sets of fractional orders, and we show the evidence as in Figure 9.

For Experiment B, we consider system changes at different fractional orders and different time delays. When $\tau_1 = \tau_2 = \cdots = \tau_n = \tau$, MFNNMD with multidelay can be treated as a single MFNNMD, as explained in Experiment A. Indeed, neurons may have varying communication delays, necessitating the consideration of varied delays in neural networks. Three examples with different values of fractional orders are given with different values of time delays. Figures 10(a) and 10(b) show that the system becomes chaotic, and Figure 10(c) shows that the systems start to become unstable and lose their chaotic characteristics. The summarization for Experiment B is shown in Table 2. All the dynamic errors with different fractional orders and time delay values show the same performance as with the fixed time delays. The error function reduces first, then increases, and eventually decreases over time. Finally, detailed time taken for dynamic errors converging to zero for Experiments A and B are shown in Tables 3 and 4.

We choose alpha = [0.995, 0.990, 0.985, 0.980, 0.975, 0.970, 0.965, 0.960] because based on the previous study, these values are most stable compared to other values of alpha. Besides, a fractional-order chaotic system will show chaotic characteristics when the alpha value is 0.95 and above. We decided to choose it and run the test on MATLAB

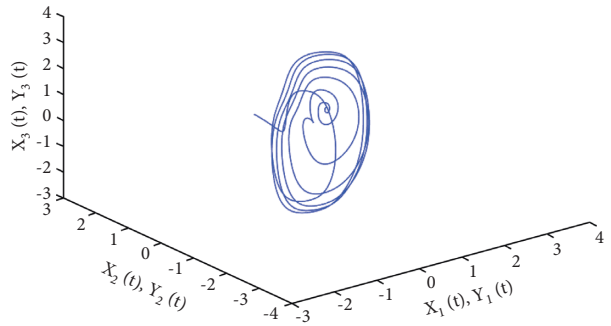

Figure 1: Experiment A: phase portrait of the chaotic attractor of MFNNMD systems (21) and (22).

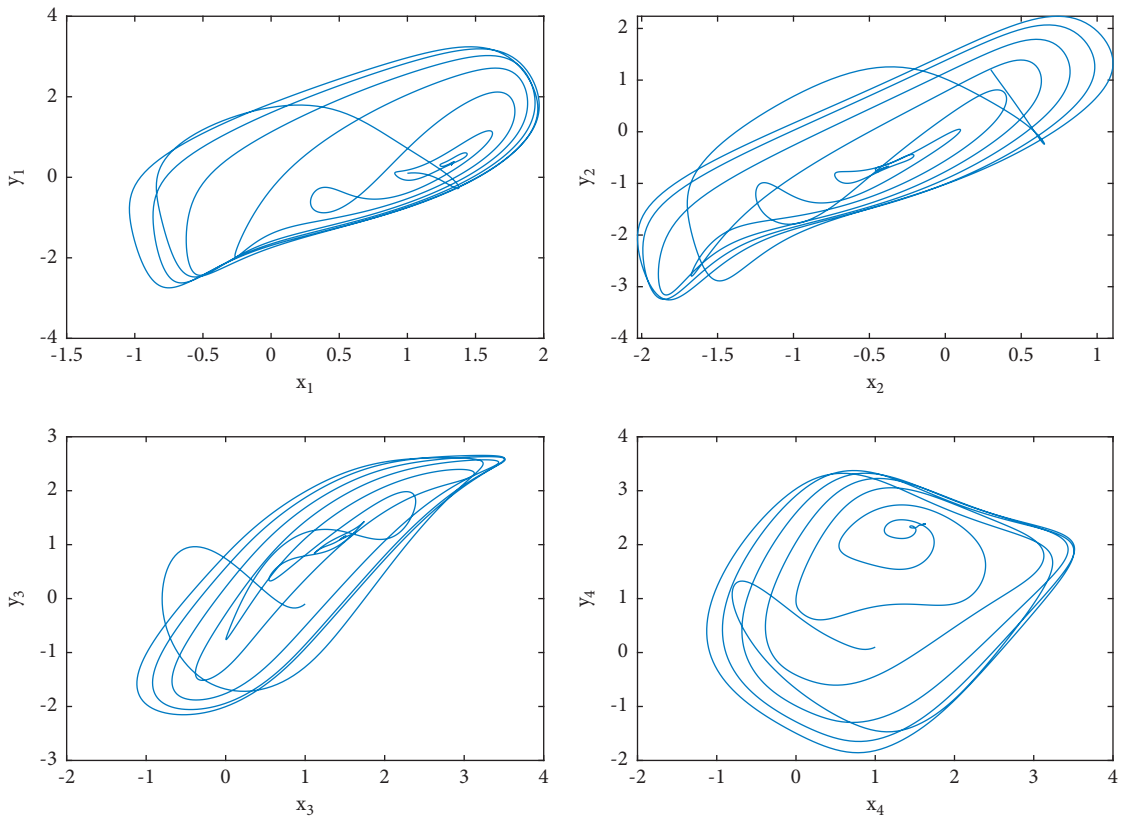

Figure 2: Experiment A: phase portrait of the X and Y of MFNNMD systems (21) and (22), when $\tau = 0.11$ and alpha = [0.995, 0.990, 0.985, 0.980, 0.975, 0.970, 0.965, 0.960].

to verify it, and we found that the error synchronization approaches zero when the systems are synchronized with each other. We also tried to run MATLAB with different alpha values, summarized the system's error synchronization in Table 2, and provided the figures as the systems start to lose their chaotic characteristics when the value of alpha decreases. These are shown in Figures 6 and 10. Besides, the main objective of our paper is to prove that with different values of alpha and time delay, there exists a chaos synchronization. Moreover, we prove that chaos synchronization occurs with the proposed control function introduced in the paper.

Besides, we choose $\tau = [0.10, 0.11, 0.12, 0.13, 0.14, 0.15, 0.16, 0.17]$ for practicability of calculation. In fact, the value of τ can be of any amount as long as the chaos characteristics are not lost. Some problems are hard for computers because of the number of combinations or the size of the data. Hence, they are chosen to solve them efficiently and avoid incorrect computations in results. We also show that these parameters show the chaotic behavior from Figures 5 and 6.

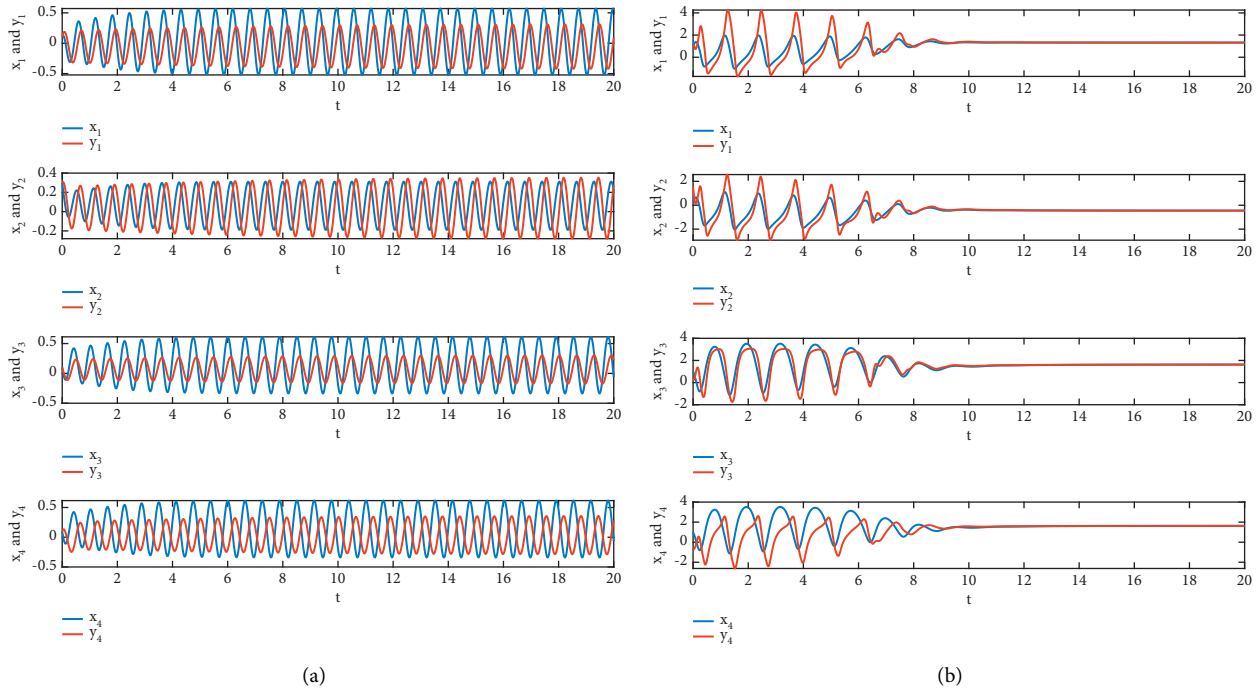

Figure 3: Experiment A: state trajectories of MFNNMD systems (21) and (22). (a) Without control activation. (b) With control activation.

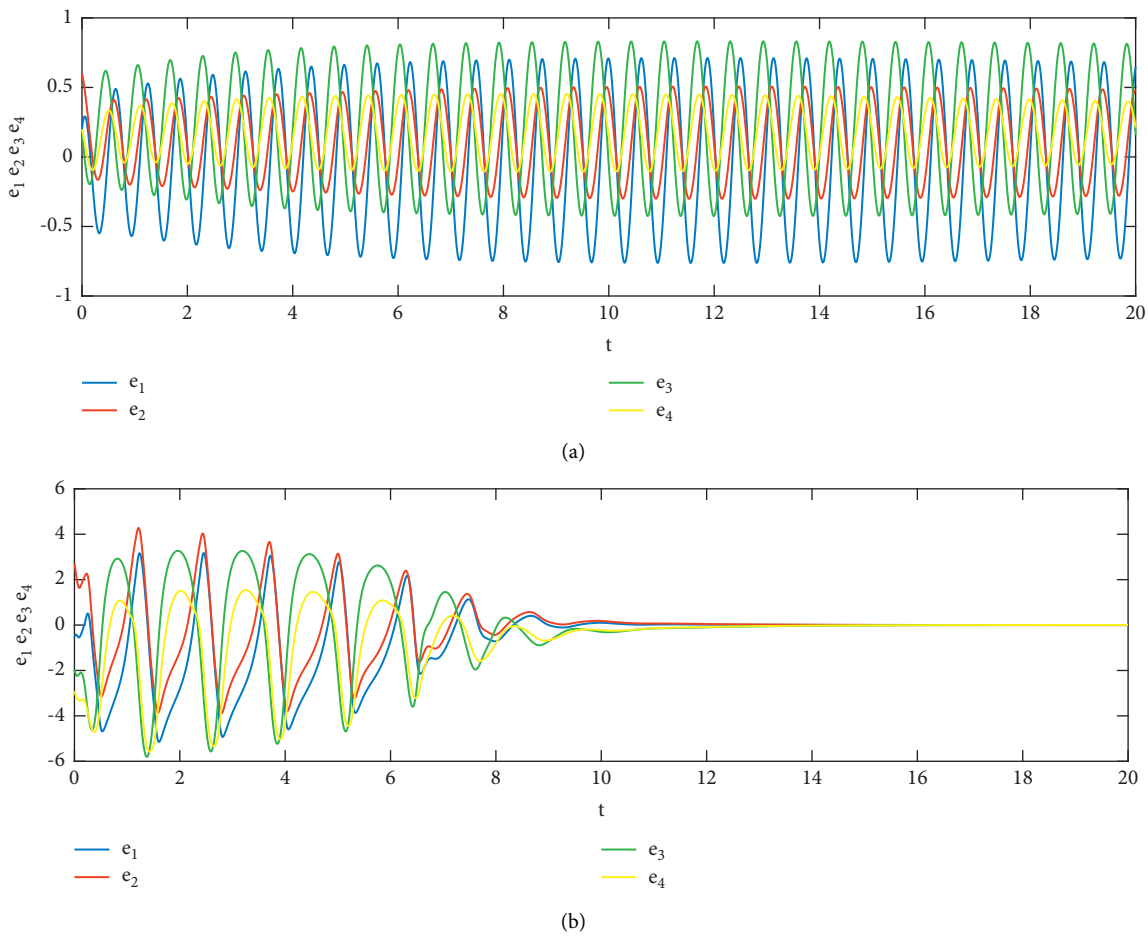

Figure 4: Experiment A: error trajectories of MFNNMD systems (21) and (22). (a) Without control activation. (b) With control activation.

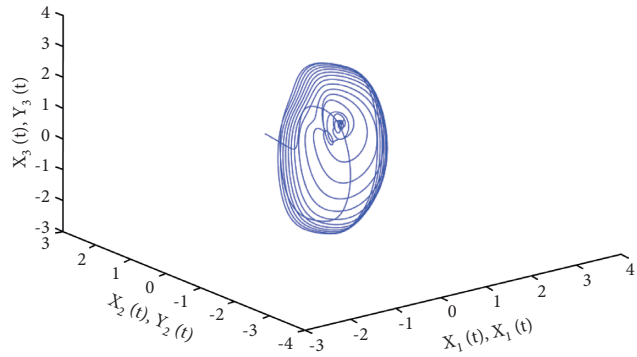

Figure 5: Experiment B: phase portrait of the chaotic attractor of MFNNMD systems (21) and (22).

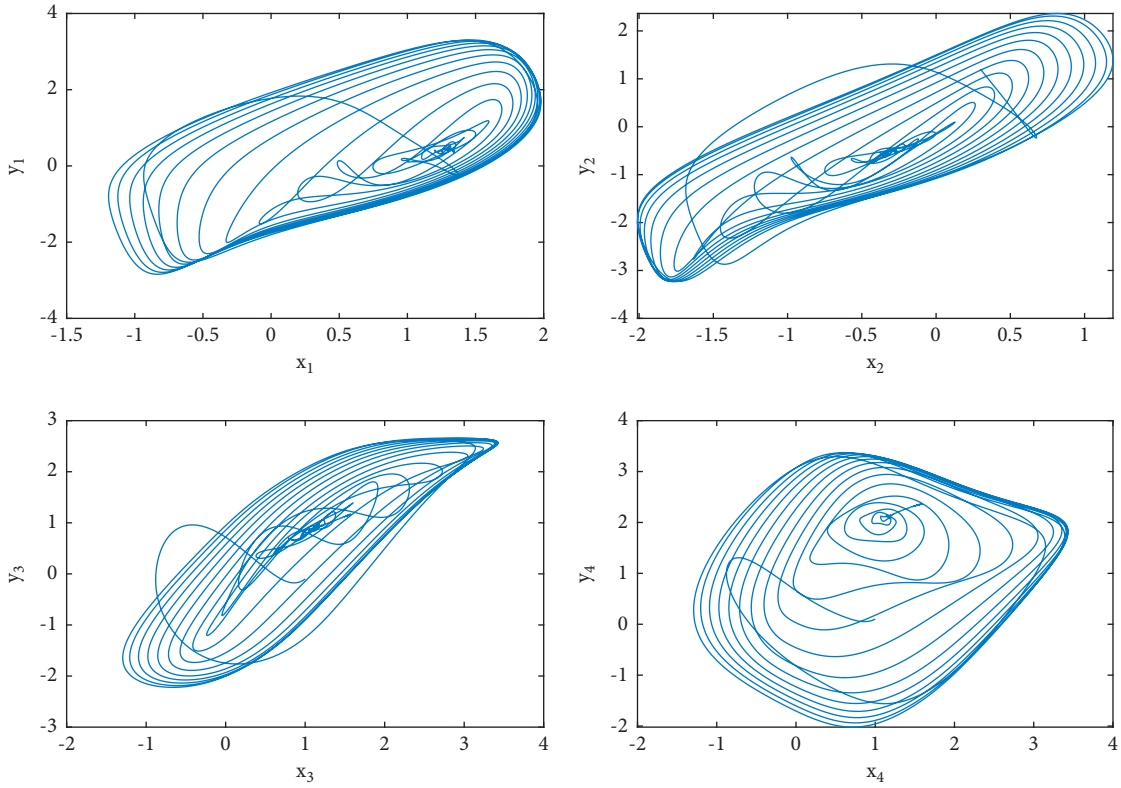

Figure 6: Experiment B: phase portrait of X and Y of MFNNMD systems (21) and (22), when τ = [0.10, 0.11, 0.12, 0.13, 0.14, 0.15, 0.16, 0.17] and alpha = [0.995, 0.990, 0.985, 0.980, 0.975, 0.970, 0.965, 0.960].

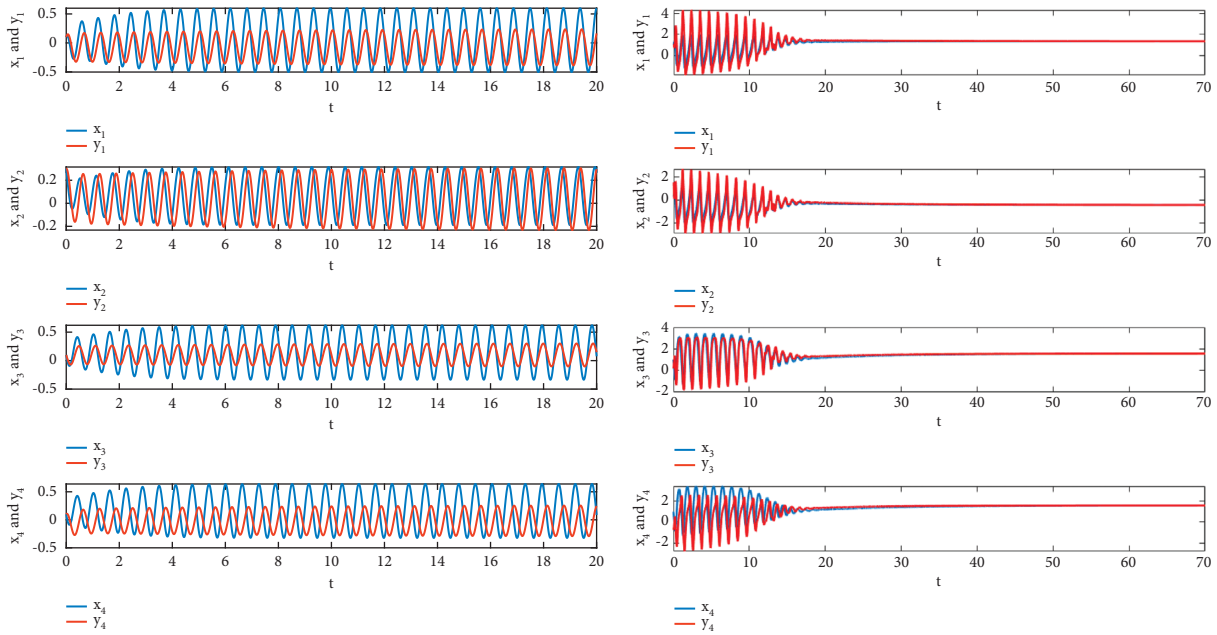

Figure 7: Experiment B: state trajectories of MFNNMD systems (21) and (22). (a) Without control activation. (b) With control activation.

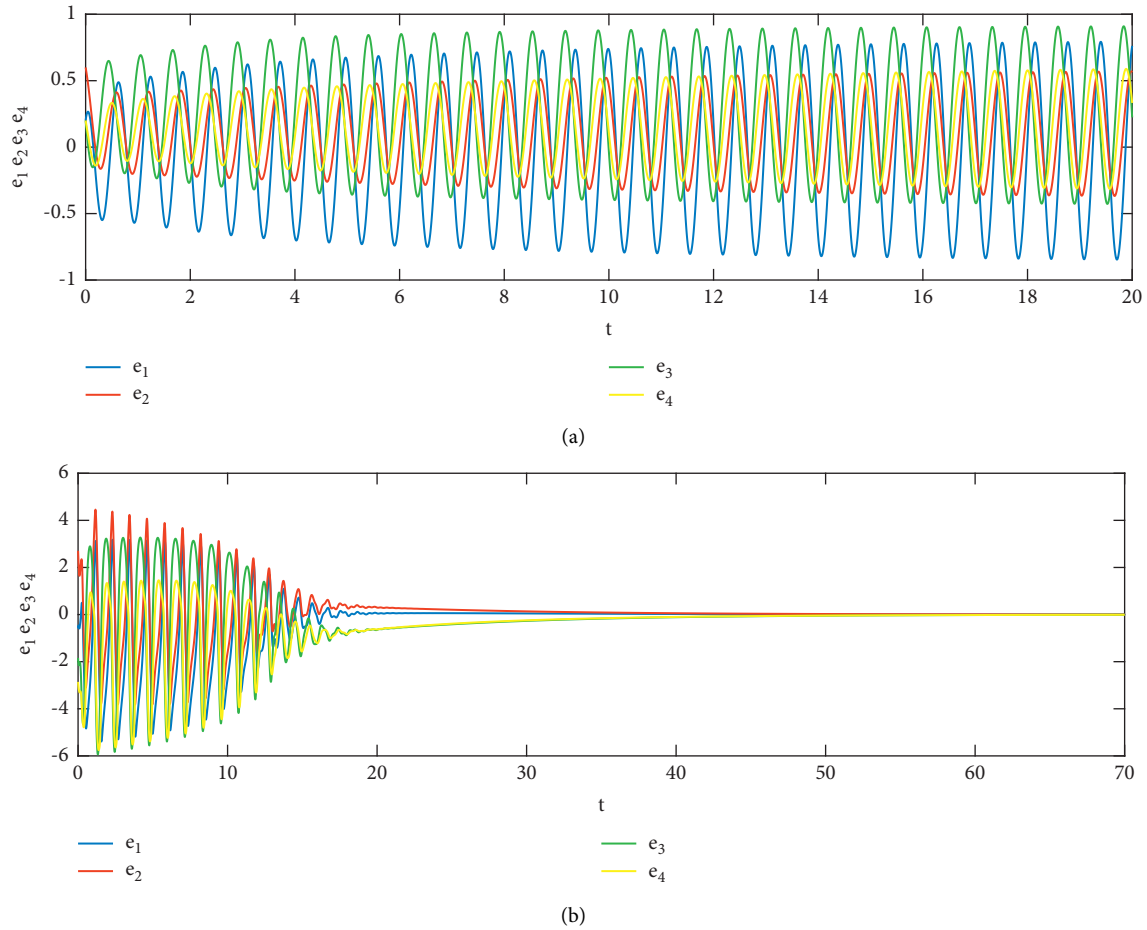

Figure 8: Experiment B: error trajectories of MFNNMD systems (21) and (22). (a) Without control activation. (b) With control activation.

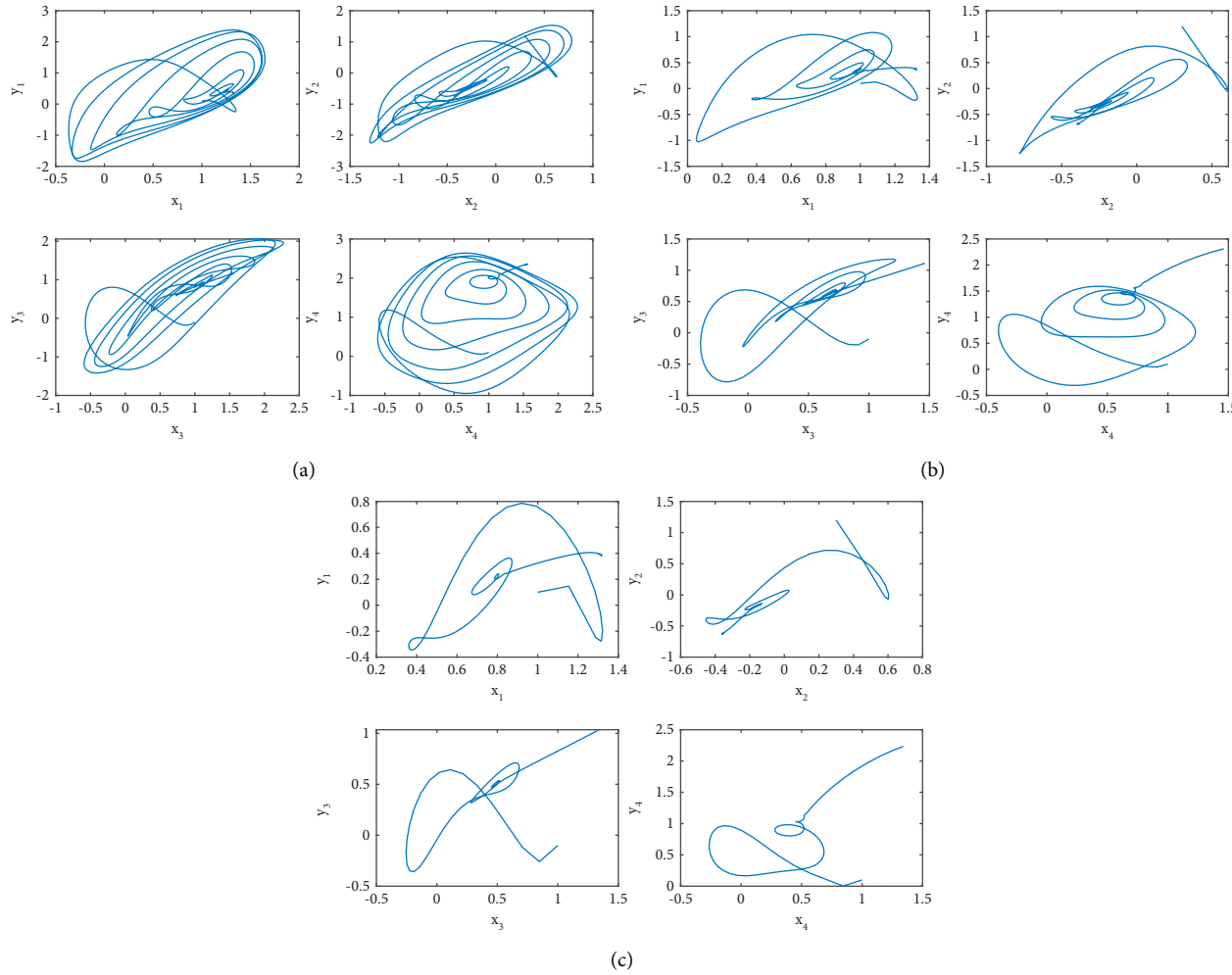

Figure 9: Phase portrait of synchronization of MFNNMD systems (21) and (22) when $\tau = 0.11$: (a) alpha = [0.895, 0.890, 0.885, 0.880, 0.875, 0.870, 0.865, 0.860], (b) alpha = [0.795, 0.790, 0.785, 0.780, 0.775, 0.770, 0.765, 0.760], and (c) alpha = [0.695, 0.690, 0.685, 0.680, 0.675, 0.670, 0.665, 0.660].

Table 1: Dynamic errors for various values of alpha (α) and $\tau = 0.11$.

Value of alpha	t	$\mathbf{e}_1$	$\mathbf{e}_2$	$\mathbf{e}_3$	$\mathbf{e}_4$
	0.2	0.124658	2.168321	−2.763986	−3.362894
$\alpha_1 = 0.995$	0.4	−2.401059	−1.517229	−3.991367	−4.667138
$\alpha_2 = 0.990$	0.6	−4.364460	−2.557856	1.480212	−1.060209
$\alpha_3 = 0.985$	0.8	−3.045370	−1.141878	2.916864	0.961262
$\alpha_4 = 0.980$	1.0	−0.889277	1.038721	2.009267	0.697992
$\alpha_5 = 0.975$	1.2	2.848753	4.206538	−2.248520	−1.196980
$\alpha_6 = 0.970$	1.4	−0.405743	−0.055542	−5.719650	−5.521897
$\alpha_7 = 0.965$	1.6	−5.144471	−3.832519	−0.562004	−3.244713
$\alpha_8 = 0.960$	1.8	−3.941395	−2.244955	2.778412	0.520882
	2.0	−2.816576	−1.176782	3.246707	1.502449
	0.2	0.121047	1.547881	−3.908083	−3.985490
$\alpha_1 = 0.895$	0.4	−3.456733	−1.662745	0.398536	−1.882546
$\alpha_2 = 0.890$	0.6	−0.866910	1.064361	1.021344	−0.378369
$\alpha_3 = 0.885$	0.8	1.628960	2.425840	−4.054332	−3.501186
$\alpha_4 = 0.880$	1.0	−3.634861	−2.180439	−0.506693	−2.636411
$\alpha_5 = 0.875$	1.2	−1.890809	−0.227439	1.540518	−0.197372
$\alpha_6 = 0.870$	1.4	1.414375	2.816090	−1.083584	−0.738211
$\alpha_7 = 0.865$	1.6	−1.924365	−1.241058	−3.434225	−4.093808
$\alpha_8 = 0.860$	1.8	−2.284485	−0.842659	1.033461	−0.840626
	2.0	−0.194050	1.222820	0.563513	−0.229726

Table 1: Continued.

Value of alpha	t	$\mathbf{e}_1$	$\mathbf{e}_2$	$\mathbf{e}_3$	$\mathbf{e}_4$
	0.2	−2.602491	−0.940676	−1.924003	−3.521095
$\alpha_1 = 0.795$	0.4	0.209412	1.830452	−1.281248	−1.679577
$\alpha_2 = 0.790$	0.6	−1.436765	0.027426	−1.132682	−2.296571
$\alpha_3 = 0.785$	0.8	0.058771	1.260416	−1.964939	−2.089092
$\alpha_4 = 0.780$	1.0	−0.882070	0.379702	−1.004009	−1.839316
$\alpha_5 = 0.775$	1.2	−0.348953	0.717825	−1.659654	−1.952206
$\alpha_6 = 0.770$	1.4	−0.523344	0.531580	−1.125355	−1.656581
$\alpha_7 = 0.765$	1.6	−0.355209	0.581332	−1.355911	−1.682493
$\alpha_8 = 0.760$	1.8	−0.379422	0.508523	−1.144286	−1.526037
	2.0	−0.292112	0.519874	−1.172738	−1.468346
	0.2	−0.836829	0.855342	−1.077397	−2.142311
$\alpha_1 = 0.695$	0.4	−0.760679	0.667618	−1.321963	−2.095273
$\alpha_2 = 0.690$	0.6	−0.676870	0.599926	−1.329555	−1.973587
$\alpha_3 = 0.685$	0.8	−0.598096	0.566648	−1.282252	−1.845552
$\alpha_4 = 0.680$	1.0	−0.536008	0.536812	−1.225057	−1.731554
$\alpha_5 = 0.675$	1.2	−0.484728	0.508685	−1.171231	−1.632134
$\alpha_6 = 0.670$	1.4	−0.439769	0.483483	−1.121826	−1.543438
$\alpha_7 = 0.665$	1.6	−0.399654	0.460903	−1.075778	−1.462798
$\alpha_8 = 0.660$	1.8	−0.363713	0.440376	−1.032476	−1.388736
	2.0	−0.331408	0.421524	−0.991581	−1.320280

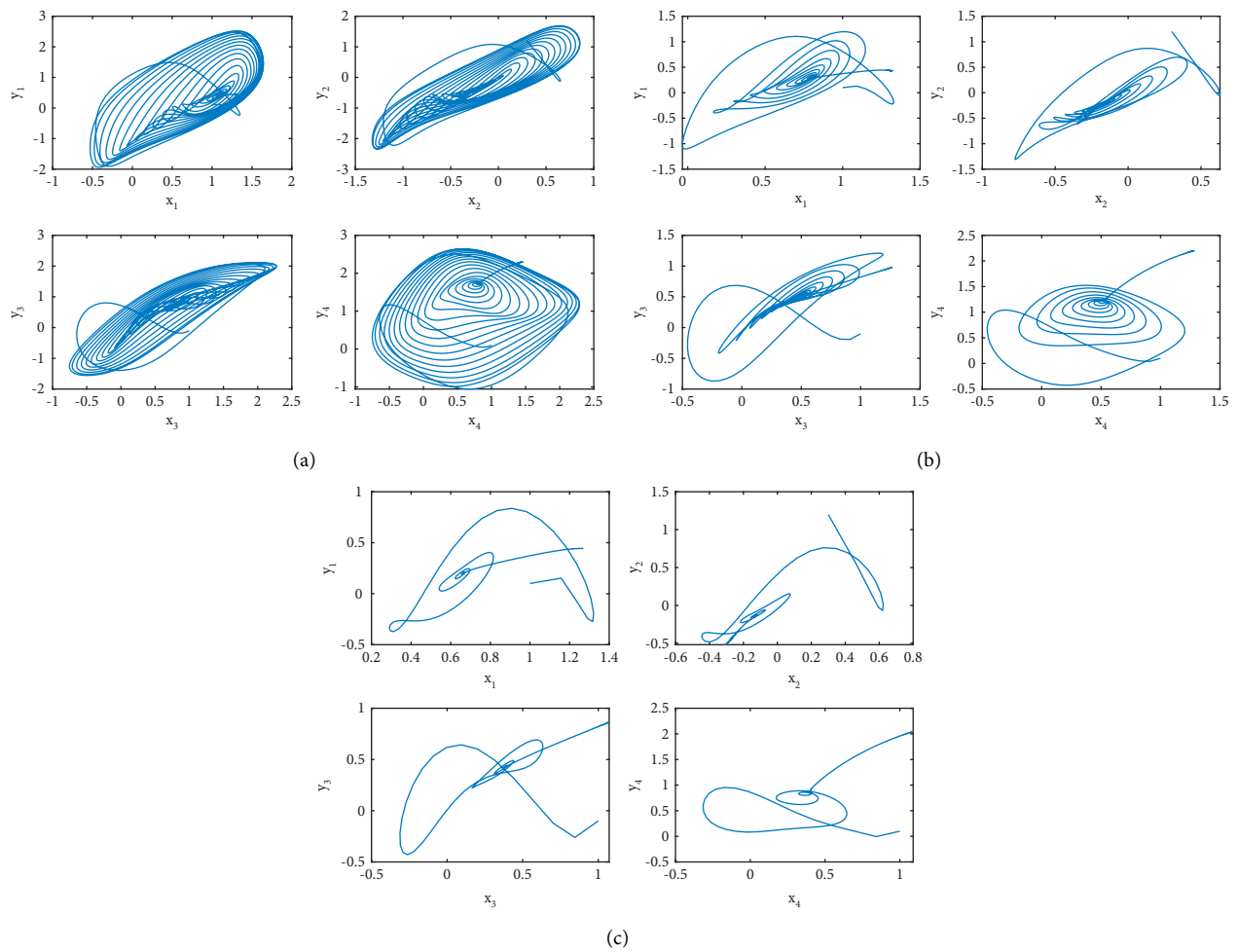

Figure 10: Phase portrait of synchronization of MFNNMD systems (21) and (22) when τ = [0.10, 0.11, 0.12, 0.13, 0.14, 0.15, 0.16, 0.17]: (a) alpha = [0.895, 0.890, 0.885, 0.880, 0.875, 0.870, 0.865, 0.860], (b) alpha = [0.795, 0.790, 0.785, 0.780, 0.775, 0.770, 0.765, 0.760], and (c) alpha = [0.695, 0.690, 0.685, 0.680, 0.675, 0.670, 0.665, 0.660].

Table 2: Dynamic errors for various values of alpha (α) and $\tau = [0.10, 0.11, 0.12, 0.13, 0.14, 0.15, 0.16, 0.17]$.

Value of alpha	t	$\mathbf{e}_1$	$\mathbf{e}_2$	$\mathbf{e}_3$	$\mathbf{e}_4$
	0.2	−2.022495	−0.065686	2.853049	1.205545
$\alpha_1 = 0.995$	0.4	−4.080703	−2.293218	2.687597	0.311466
$\alpha_2 = 0.990$	0.6	−1.320927	−1.122006	−5.013653	−5.232768
$\alpha_3 = 0.985$	0.8	−0.214395	1.082445	1.686627	0.853142
$\alpha_4 = 0.980$	1.0	−2.728065	−1.613715	2.429691	0.460877
$\alpha_5 = 0.975$	1.2	−2.354545	−1.618750	−1.338532	−2.756335
$\alpha_6 = 0.970$	1.4	−0.410080	0.051628	−1.815041	−1.838976
$\alpha_7 = 0.965$	1.6	−0.134854	0.233707	−1.195806	−1.213489
$\alpha_8 = 0.960$	1.8	0.002574	0.298025	−0.846826	−0.835130
	2.0	0.051801	0.297613	−0.650303	−0.630223
	0.2	0.940363	2.652079	−0.323689	−0.373100
$\alpha_1 = 0.895$	0.4	1.032723	2.446092	−0.593181	−0.486812
$\alpha_2 = 0.890$	0.6	1.516537	2.179133	−2.695674	−2.141750
$\alpha_3 = 0.885$	0.8	−1.193599	−0.160199	−1.124218	−1.989497
$\alpha_4 = 0.880$	1.0	−0.095008	0.720590	−0.875975	−1.115168
$\alpha_5 = 0.875$	1.2	−0.187524	0.466583	−1.086851	−1.240937
$\alpha_6 = 0.870$	1.4	−0.150788	0.407471	−0.926858	−1.065040
$\alpha_7 = 0.865$	1.6	−0.102513	0.370933	−0.828564	−0.929539
$\alpha_8 = 0.860$	1.8	−0.067105	0.336450	−0.742594	−0.814420
	2.0	−0.040825	0.304890	−0.665046	−0.714429
	0.2	−0.628486	0.752827	−1.065626	−1.705763
$\alpha_1 = 0.795$	0.4	−0.616681	0.508169	−1.175186	−1.674920
$\alpha_2 = 0.790$	0.6	−0.501480	0.455924	−1.084421	−1.493109
$\alpha_3 = 0.785$	0.8	−0.413107	0.413356	−0.992929	−1.334976
$\alpha_4 = 0.780$	1.0	−0.341905	0.377650	−0.910913	−1.198937
$\alpha_5 = 0.775$	1.2	−0.283942	0.346661	−0.836579	−1.080232
$\alpha_6 = 0.770$	1.4	−0.236418	0.319153	−0.768815	−0.975700
$\alpha_7 = 0.765$	1.6	−0.197244	0.294346	−0.706797	−0.883013
$\alpha_8 = 0.760$	1.8	−0.164814	0.271723	−0.649864	−0.800362
	2.0	−0.137868	0.250926	−0.597470	−0.726300
	0.2	−0.726436	0.450155	−0.988908	−1.560065
$\alpha_1 = 0.695$	0.4	−0.607764	0.387185	−0.887064	−1.357983
$\alpha_2 = 0.690$	0.6	−0.520729	0.344249	−0.808443	−1.210932
$\alpha_3 = 0.685$	0.8	−0.451719	0.310852	−0.741817	−1.091060
$\alpha_4 = 0.680$	1.0	−0.395014	0.283278	−0.683254	−0.988966
$\alpha_5 = 0.675$	1.2	−0.347410	0.259682	−0.630746	−0.899911
$\alpha_6 = 0.670$	1.4	−0.306854	0.238995	−0.583070	−0.821019
$\alpha_7 = 0.665$	1.6	−0.271920	0.220533	−0.539396	−0.750353
$\alpha_8 = 0.660$	1.8	−0.241567	0.203835	−0.499119	−0.686514
	2.0	−0.215007	0.188574	−0.461779	−0.628448

Table 3: Error dynamics of MFNNMD time taken for the system to converge to zero at 12.5 s.

t	$\mathbf{e}_1$	$\mathbf{e}_2$	$\mathbf{e}_3$	$\mathbf{e}_4$
0.5	−4.543203	−3.139601	−0.945464	−3.280529
1.0	−0.889277	1.038721	2.009267	0.697992
1.5	−3.304613	−2.685071	−3.987378	−5.315820
2.0	−2.816576	−1.176782	3.246707	1.502449
2.5	2.721507	3.151517	−4.530053	−3.481734
3.0	−3.859544	−2.409818	2.681677	0.432567
3.5	−0.254657	1.163567	1.698179	0.839844
4.0	−3.870729	−3.410456	−2.468871	−4.284681
4.5	−2.467705	−1.337839	3.105034	1.449527
5.0	2.6571946	3.142837	−2.195461	−1.082126
5.5	−3.088547	−2.128426	1.827998	−0.297806
6.0	−0.697681	0.166480	1.893956	0.911106
6.5	−1.516066	−1.314321	−2.716662	−3.184804
7.0	−1.203530	−0.667153	1.428096	0.132208

Table 3: Continued.

t	$\mathbf{e}_1$	$\mathbf{e}_2$	$\mathbf{e}_3$	$\mathbf{e}_4$
7.5	1.119343	1.305388	−1.469884	−0.739766
8.0	−0.711474	−0.424856	−0.134413	−0.805776
8.5	0.280983	0.492073	−0.270894	−0.141005
9.0	0.000535	0.142655	−0.714078	−0.668082
9.5	−0.025467	0.097831	−0.166414	−0.245520
10.0	0.101626	0.181401	−0.299729	−0.226463
11.5	0.028709	0.062857	−0.127231	−0.108899
12.0	0.020033	0.045478	−0.101927	−0.088572
12.5	0.014275	0.033330	−0.074386	−0.065294
13.0	0.011821	0.025848	−0.056715	−0.048516
13.5	0.009202	0.019420	−0.043685	−0.036732
14.0	0.006896	0.014234	−0.032887	−0.027252
14.5	0.005236	0.010356	−0.024558	−0.019813
15.0	0.003951	0.007358	−0.018224	−0.014137
15.5	0.002916	0.004999	−0.013279	−0.009730
16.0	0.002105	0.003155	−0.009405	−0.006271
16.5	0.001471	0.001710	−0.006375	−0.003556
17.0	0.000969	0.000569	−0.003990	−0.001413
17.5	0.000570	−0.000338	−0.002098	0.000291
18.0	0.000251	−0.001064	−0.000589	0.001658
18.5	−5.147413	−0.001651	0.000624	0.002762
19.0	−0.000213	−0.002128	0.001609	0.003663
19.5	−0.000384	−0.002521	0.002415	0.004405
20.0	−0.000525	−0.002847	0.003082	0.005023

Table 4: Error dynamics of MFNNMD time taken for the system to converge to zero at 42.0 s.

t	$\mathbf{e}_1$	$\mathbf{e}_2$	$\mathbf{e}_3$	$\mathbf{e}_4$
2.0	−2.022495	−0.065686	2.853049	1.205545
4.0	−4.080703	−2.293218	2.687597	0.311466
6.0	−1.320927	−1.122006	−5.013653	−5.232768
8.0	−0.214395	1.082445	1.686627	0.853142
10.0	−2.728065	−1.613715	2.429691	0.460877
12.0	−2.354545	−1.618750	−1.338532	−2.756335
14.0	−0.410080	0.051628	−1.815041	−1.838976
16.0	−0.134854	0.233707	−1.195806	−1.213489
18.0	0.002574	0.298025	−0.846826	−0.835130
20.0	0.051801	0.297613	−0.650303	−0.630223
22.0	0.059929	0.260617	−0.534643	−0.512342
24.0	0.060217	0.222786	−0.450020	−0.424671
26.0	0.057451	0.189368	−0.378857	−0.352509
28.0	0.052952	0.160436	−0.318578	−0.293027
30.0	0.047683	0.135605	−0.267669	−0.243969
32.0	0.042246	0.114409	−0.224808	−0.203483
34.0	0.037000	0.096395	−0.188799	−0.170031
36.0	0.032138	0.081131	−0.158585	−0.142347
38.0	0.027746	0.068226	−0.133245	−0.119397
40.0	0.023848	0.057329	−0.111995	−0.100333
42.0	0.020428	0.048135	−0.094166	−0.084467
44.0	0.017455	0.040379	−0.079199	−0.071235
46.0	0.014886	0.033835	−0.066623	−0.060178
48.0	0.012674	0.028311	−0.056043	−0.050918
50.0	0.010777	0.023645	−0.047133	−0.043149
52.0	0.009152	0.019700	−0.039617	−0.036617
54.0	0.007763	0.016360	−0.033269	−0.031113
56.0	0.006575	0.013529	−0.027897	−0.026465
58.0	0.005559	0.011126	−0.023343	−0.022532
60.0	0.004690	0.009082	−0.019476	−0.019197
62.0	0.003946	0.007340	−0.016184	−0.016360
64.0	0.003308	0.005853	−0.013377	−0.013943
66.0	0.002760	0.004580	−0.010976	−0.011877
68.0	0.002289	0.003488	−0.008918	−0.010107
70.0	0.001883	0.002548	−0.007148	−0.008585

5. Conclusions

The chaos synchronization of MFNNMD is evaluated in this article. The conditions for synchronization of MFNNMD systems are examined using FLDM and sliding mode techniques. We have demonstrated that MFNNMD systems can archive chaos synchronization with distinct fractional orders when the parameters and beginning conditions are fixed. Numerical simulations are used to authenticate the suggested technique's feasibility and effectiveness. It has been demonstrated that the provided strategy is capable of ensuring that all error signals converge to zero and remain within the system. Then, an example of graphical results is given to authenticate our proposed method's effectiveness. Finally, the impacts of multi-fractional order and multi-time delay on synchronization are addressed in greater detail. In addition, we anticipate some applications to the actual world that relate to secure communication.

Data Availability

The data used to support the findings of this study are included within the article.

Conflicts of Interest

The authors declare no conflicts of interest.

Acknowledgments

All authors were partially funded by Universiti Malaya under grant no. IIRG001C-2019.

Supplementary Materials

The annex contains a MATLAB code named MFNNMDNocontrolnew. (*Supplementary Materials*)

References

[1] J.-H. He, "Approximate analytical solution for seepage flow with fractional derivatives in porous media," *Computer Methods in Applied Mechanics and Engineering*, vol. 167, no. 1–2, pp. 57–68, 1998.

[2] K. S. Miller and B. Ross, *An Introduction to the Fractional Calculus and Fractional Differential Equations*, John Wiley & Sons, Nashville, TN, 1993.

[3] E. Goldfain, "Fractional dynamics and the Standard Model for particle physics," *Communications in Nonlinear Science and Numerical Simulation*, vol. 13, no. 7, pp. 1397–1404, 2008.

[4] R. E. Gutiérrez, J. M. Rosário, and J. Tenreiro Machado, "Fractional order calculus: basic concepts and engineering applications," *Mathematical Problems in Engineering*, vol. 2010, Article ID 375858, 19 pages, 2010.

[5] S. G. Samko, A. A. Kilbas, and O. I. Marichev, "Fractional integrals and derivatives and some of their applications," *Sci-Tech*, vol. 1, 1987.

[6] K. Diethelm, *The Analysis of Fractional Differential Equations: An Application-Oriented Exposition Using Differential Operators of Caputo Type*, Springer, Berlin, Germany, 2010th edition, 2010.

[7] X. J. Yang, *Advanced Local Fractional Calculus and its Applications*, World Science, New York, USA, 2012.

[8] C. Cattani, H. M. Srivastava, and X. J. Yang, *Fractional Dynamics*, De Gruyter, Berlin, Germany, 2019.

[9] X. Chen, J. H. Park, J. Cao, and J. Qiu, "Adaptive synchronization of multiple uncertain coupled chaotic systems via sliding mode control," *Neurocomputing*, vol. 273, pp. 9–21, 2018.

[10] M. Asadollahi, A. R. Ghiasi, and M. A. Badamchizadeh, "Adaptive synchronization of chaotic systems with hysteresis quantizer input," *ISA Transactions*, vol. 98, pp. 137–148, 2020.

[11] H. Xi, Y. Li, and X. Huang, "Adaptive function projective combination synchronization of three different fractional-order chaotic systems," *Optik*, vol. 126, no. 24, pp. 5346–5349, 2015.

[12] O. Garcia-Sepúlveda, C. Posadas-Castillo, A. D. Cortés-Preciado, M. A. Platas-Garza, E. Garza-González, and A. G. S. Sanchez, "Synchronization of fractional-order Lü chaotic oscillators for voice encryption," *Revista Mexicana de Física*, vol. 66, no. 3, pp. 364–371, 2020.

[13] H. Ahmed, I. Salgado, and H. Rios, "Robust synchronization of master-slave chaotic systems using approximate model: an experimental study," *ISA Transactions*, vol. 73, pp. 141–146, 2018.

[14] C. Hu, J. Yu, Z. Chen, H. Jiang, and T. Huang, "Fixed-time stability of dynamical systems and fixed-time synchronization of coupled discontinuous neural networks," *Neural Networks*, vol. 89, pp. 74–83, 2017.

[15] A. Polyakov, "Nonlinear feedback design for fixed-time stabilization of linear control systems," *IEEE Transactions on Automatic Control*, vol. 57, no. 8, pp. 2106–2110, 2012.

[16] A. Polyakov, D. Efimov, and W. Perruquetti, "Finite-time and fixed-time stabilization: implicit Lyapunov function approach," *Automation*, vol. 51, pp. 332–340, 2015.

[17] J. Hu and G. Sui, "Fixed-time control of static impulsive neural networks with infinite distributed delay and uncertainty," *Communications in Nonlinear Science and Numerical Simulation*, vol. 78, Article ID 104848, 2019.

[18] L. M. Pecora and T. L. Carroll, "Synchronization in chaotic systems," *Physical Review Letters*, vol. 64, no. 8, pp. 821–824, 1990.

[19] J. Yu, C. Hu, H. Jiang, and X. Fan, "Projective synchronization for fractional neural networks," *Neural Networks*, vol. 49, pp. 87–95, 2014.

[20] G. Peng, Y. Jiang, and F. Chen, "Generalized projective synchronization of fractional order chaotic systems," *Phys. A Stat. Mech. its Appl.*vol. 387, no. 14, 2008.

[21] H. Bao, J. H. Park, and J. Cao, "Adaptive synchronization of fractional-order memristor-based neural networks with time delay," *Nonlinear Dynamics*, vol. 82, no. 3, 2015.

[22] Z. Ding and Y. Shen, "Projective synchronization of non-identical fractional-order neural networks based on sliding mode controller," *Neural Networks*, vol. 76, 2016.

[23] A. Ouannas, G. Grassi, T. Ziar, and Z. Odibat, "On a function projective synchronization scheme for non-identical Fractional-order chaotic (hyperchaotic) systems with different dimensions and orders," *Optik*, vol. 136, pp. 513–523, 2017.

[24] H. B. Bao and J. De Cao, "Projective synchronization of fractional-order memristor-based neural networks," *Neural Networks*, vol. 63, pp. 1–9, 2015.

[25] J. Lu and G. Chen, "A time-varying complex dynamical network model and its controlled synchronization criteria," *IEEE Transactions on Automatic Control*, vol. 50, no. 6, pp. 841–846, 2005.

[26] X. Zhang, X. Zhang, D. Li, and D. Yang, "Adaptive synchronization for a class of fractional order time-delay uncertain chaotic systems via fuzzy fractional order neural network," *International Journal of Control, Automation, and Systems*, vol. 17, no. 5, pp. 1209–1220, 2019.

[27] A.-B. A. Al-Hussein, F. Rahma, and S. Jafari, "Hopf bifurcation and chaos in time-delay model of glucose-insulin regulatory system," *Chaos, Solitons & Fractals*, vol. 137, Article ID 109845, 2020.

[28] J. K. Hale and S. M. Verduyn Lunel, *Introduction to Functional Differential Equations*, Springer, Berlin, Germany, 3rd edition, 1993.

[29] W. Deng, Y. Wu, and C. Li, "Stability analysis of differential equations with time-dependent delay," *Int. J. Bifurcat. Chaos*, vol. 16, no. 2, pp. 465–472, 2006.

[30] C.-K. Cheng, H.-H. Kuo, Y.-Y. Hou, C.-C. Hwang, and T.-L. Liao, "Robust chaos synchronization of noise-perturbed chaotic systems with multiple time-delays," *Physica A*, vol. 387, no. 13, pp. 3093–3102, 2008.

[31] Y. Xiao, W. Xu, S. Tang, and X. Li, "Adaptive complete synchronization of the noise-perturbed two bi-directionally coupled chaotic systems with time-delay and unknown parametric mismatch," *Applied Mathematics and Computation*, vol. 213, no. 2, pp. 538–547, 2009.

[32] W. He, F. Qian, J. Cao, and Q.-L. Han, "Impulsive synchronization of two nonidentical chaotic systems with time-varying delay," *Physics Letters A*, vol. 375, no. 3, pp. 498–504, 2011.

[33] J.-P. Richard, "Time-delay systems: an overview of some recent advances and open problems," *Automatica*, vol. 39, no. 10, pp. 1667–1694, 2003.

[34] X. Li and M. Bohner, "Exponential synchronization of chaotic neural networks with mixed delays and impulsive effects via output coupling with delay feedback," *Mathematical and Computer Modelling*, vol. 52, no. 5–6, pp. 643–653, 2010.

[35] S. Samanta, P. K. Tiwari, A. K. Alzahrani, and A. S. Alshomrani, "Chaos in a nonautonomous eco-epidemiological model with delay," *Applied Mathematical Modelling*, vol. 79, pp. 865–880, 2020.

[36] F. N. A. Latiff, W. A. M. Othman, and N. Kumaresan, "Synchronization OF delayed integer order and delayed fractional order recurrent neural networks system with active sliding mode," *International Transaction Journal of Engineering, Management, & Applied Sciences & Technologies*, vol. 11, no. 12, pp. 1–15, 2020.

[37] X. Li, X. Yang, and S. Song, "Lyapunov conditions for finite-time stability of time-varying time-delay systems," *Automatica*, vol. 103, pp. 135–140, 2019.

[38] S. S. Ge, F. Hong, and T. H. Lee, "Adaptive neural control of nonlinear time-delay systems with unknown virtual control coefficients," *IEEE Transactions on Systems, Man, and Cybernetics - Part B: Cybernetics*, vol. 34, no. 1, pp. 499–516, 2004.

[39] S. S. Ge, F. Hong, and T. H. Lee, "Robust adaptive control of nonlinear systems with unknown time delays," in *Proceedings of the 2004 (IEEE) International Symposium on Intelligent Control*, Taipei, Taiwan, January 2005.

[40] I. Podlubny, "Fractional Differential Equations," *An Introduction to Fractional Derivatives, Fractional Differential Equations, To Methods of Their*, Vol. 198, Academic press, Cambridge, Massachusetts, United States, 1998.

[41] Y. Wei, Y. Chen, T. Liu, and Y. Wang, "Lyapunov functions for nabla discrete fractional order systems," *ISA Transactions*, vol. 88, pp. 82–90, 2019.

[42] I. Stamova and G. Stamov, "Mittag-Leffler synchronization of fractional neural networks with time-varying delays and reaction–diffusion terms using impulsive and linear controllers," *Neural Networks*, vol. 96, pp. 22–32, Dec. 2017.

[43] S. Bhalekar and V. Daftardar-Gejji, "Fractional ordered Liu system with time-delay," *Communications in Nonlinear Science and Numerical Simulation*, vol. 15, no. 8, pp. 2178–2191, 2010.